Eye (2017) 31, 578–587

www.nature.com/eye

CLINICAL STUDY

Ocular characteristics associated with the location of focal lamina cribrosa defects in open-angle glaucoma patients

H-YL Park, YS Hwang and CK Park

Abstract

Purpose **To investigate the clinical characteristics according to the location of focal lamina cribrosa (LC) defects and its associated ocular features.**

Patients and methods **A total of 139 open-angle glaucoma patients underwent Spectralis optical coherence tomography (OCT) with enhanced depth imaging. Alterations in the contour of the LC were investigated to find focal LC defects. The location of the visible LC defect from the neural canal wall (far-peripheral and mid-peripheral) and clock-hour position (superotemporal, temporal and inferotemporal) were classified. Disc ovality ratio and disc-foveal angle were measured from disc and retinal nerve fiber layer (RNFL) photographs. The disc tilt degree was measured using a Heidelberg Retina Tomograph (HRT) III system. The *en face* OCT image of the disc scans was registered to the disc and RNFL photographs, to determine whether the focal LC defects corresponded spatially to the glaucomatous damage location.**

Results **Eyes with far-peripheral LC defects were significantly myopic and had a higher disc ovality ratio. The disc tilt degree obtained by HRT revealed significant temporal disc tilt in eyes with temporal LC defects ($P<0.001$). Eyes with inferotemporal LC defects had a significantly larger disc-foveal angle ($P=0.027$). The inferotemporal LC defects corresponded to the location of glaucomatous damage in 81.6%; however, only 46.2% of eyes with a superotemporal LC defect and 3.2% of eyes with a temporal LC defect corresponded spatially with the glaucomatous damage location.**

Conclusions **The clinical characteristics and association with glaucomatous damage location were different according to the location of focal LC defect.**

Eye (2017) **31,** 578–587; doi:10.1038/eye.2016.270; published online 9 December 2016

Introduction

There are growing evidences showing the structural alterations at the level of the lamina cribrosa (LC) are important in the pathogenesis of glaucoma.[1–3] With the advent of spectral-domain optical coherence tomography (OCT) with enhanced depth imaging (EDI), we can now capture the images of the LC *in vivo*. Several studies have identified LC findings including LC thinning, posterior displacement, and changes like focal hole, focal defect, and disinsertion.[4–6]

Many studies focused to the ocular characteristics related to the presence of LC alterations. The focal LC defect or hole was reported to be associated with localized retinal nerve fiber layer (RNFL) defects, disc hemorrhages, normal-tension glaucoma (NTG) diagnosis, and myopic refractive errors.[7–10] Eyes with LC defects appeared to have more frequent paracentral scotomas compared with eyes without LC defects.[11,12] Also, the locations of LC findings were variable among previous studies. Some LC alterations have been observed in the peripheral region of the visible LC; others have been observed in the central region of the visible LC.[10,11,13] Most LC alterations are detected in the inferotemporal region, but superotemporal LC alterations and LC alterations near the nine o'clock position have also been found.[8–12,14] The clinical relevance of the presence of LC findings and the location of these LC findings has yet to be determined.

In this study, we investigate related ocular characteristics according to the presence and the

Department of Ophthalmology, Seoul St. Mary's Hospital, College of Medicine, The Catholic University of Korea, Seoul, South Korea

Correspondence:
CK Park, Department of Ophthalmology, Seoul St. Mary's Hospital, College of Medicine, The Catholic University of Korea, 505 Banpo-dong, Seocho-ku, Seoul 137-701, Korea
Tel: +82 2 2258 6199;
Fax: +82 2 533 3801.
E-mail: ckpark@catholic.ac.kr

Received: 24 February 2016
Accepted in revised form: 14 October 2016
Published online: 9 December 2016

location of the focal LC defect. Eyes with focal LC defects were compared with eyes without focal LC defects and subgroup comparisons were performed according to the location of focal LC defects.

Materials and methods

Subjects

This cross-sectional, case-control design investigated consecutive open-angle glaucoma patients who were seen by a glaucoma specialist (CKP) from January 2014 to December 2014 at the glaucoma clinic of Seoul St Mary's Hospital. This study was approved by the Institutional Review Board at Seoul St Mary's Hospital and complied with the principles outlined in the Declaration of Helsinki. Written informed consent was obtained from the participants.

Each participant underwent a comprehensive ophthalmic assessment, including measurement of best-corrected visual acuity, refraction, slit-lamp biomicroscopy, gonioscopy, Goldmann applanation tonometry, central corneal thickness using ultrasound pachymetry (Tomey Corporation, Nagoya, Japan), axial length using ocular biometry (IOL Master; Carl Zeiss Meditec, Dublin, CA, USA), dilated stereoscopic examination of the optic disc and fundus, color disc photography, red-free RNFL photography (Canon, Tokyo, Japan), Cirrus OCT (Carl Zeiss Meditec), confocal scanning laser ophthalmoscopy using the Heidelberg Retina Tomograph III (HRT III; Heidelberg Engineering, Heidelberg, Germany), Heidelberg Spectralis system (Heidelberg Engineering), and Humphrey visual field (VF) examination using the 24-2 Swedish Interactive Threshold Algorithm Standard program (Carl Zeiss Meditec).

For glaucoma diagnosis, patients had to fulfill the following criteria: glaucomatous optic disc appearences (such as diffuse or localized rim thinning, a notch in the rim, or a vertical cup-to-disc ratio higher than that of the other eye by more than 0.2) and glaucomatous VF loss (defined as a consistent presence of a cluster of ≥ 3 non-edge points on the pattern deviation plot with a probability of occurring in $<5\%$ of the normal population, with one of these points having the probability of occurring in $<1\%$ of the normal population; a pattern SD with $P<5\%$, or a Glaucoma Hemifield Test result outside the normal limits in a consistent pattern on two qualifying VFs), both confirmed by two glaucoma specialists (HYP, CKP), in addition to an open angle on gonioscopic examination.

To be included in the study, patients were required to meet the following inclusion criteria: a best-corrected visual acuity $\geq 20/40$, a spherical refraction within ± 12.0 diopters, a cylinder correction within ± 3.0 diopters, consistently reliable VFs (defined as false negative $<15\%$, false positive $<15\%$, and fixation losses $<20\%$), and a mean deviation (MD) exceeding -20.00 dB. Patients were excluded on the basis of any of the following criteria: a history of any retinal diseases; a history of eye trauma or surgery, with the exception of uncomplicated cataract surgery; other optic nerve disease besides glaucoma; or a history of systemic or neurologic diseases that might affect the VF. Only the right eye was randomly selected for the study.

Measurement of the optic disc tilt, torsion, peripapillary atrophy area, and disc-foveal angle

To quantify the anatomical profiles of the optic disc, we measured disc tilt using disc ovality ratio, disc torsion using torsion degree, peripapillary atrophy (PPA) area, disc-foveal angle using red-free RNFL photographs, and tilt degree using HRT. Measurement parameter details are described in our previous studies.[15–20]

Color disc and red-free RNFL photographs were obtained using the standard settings of a nonmydriatic retinal camera (Kowa, Tokyo, Japan). The disc photographs and red-free images were evaluated independently in random order and in a masked fashion by two of the authors (HYP and YSH). The disc ovality ratio, disc torsion degree, PPA area, and disc-foveal angle were measured on photographs using the National Institutes of Health image analysis software (ImageJ version 1.40; available at http://rsb.info.nih.gov/ij/index.html (in the public domain); developed by Wayne Rasband, National Institutes of Health, Bethesda, MD, USA; Figure 1a). The disc ovality index was determined using the tilt ratio (the ratio between the longest and shortest disc diameter). If the tilt ratio of the optic disc exceeded 1.30, then the optic disc was classified as a tilted disc.[21–23] Disc torsion refers to the deviation of the long disc axis from the vertical meridian (ie, the vertical line perpendicular to a reference line connecting the fovea and the disc center). The angle between the vertical meridian and the long axis of the disc is the degree of torsion. The optic disc was classified as a torsioned disc when the degree of torsion was more than 15°.[24,25] Positive and negative angles indicated the presence of inferotemporal and superonasal torsion, respectively. The beta zone PPA, defined as an inner crescent of chorioretinal atrophy with visible sclera and choroidal vessels, was plotted using a mouse-driven cursor to trace the disc and PPA margin directly onto the image. The pixel areas were calculated to define the PPA area. The disc-foveal angle is the angle between the optic disc and fovea as measured by the angle between the reference line and a horizontal line through the disc

center, as described previously. A positive value indicates that the fovea was located inferior to the optic disc.

The degrees of temporal and vertical disc tilt were measured using HRT III (Figure 1b).[16,26] Topographic images were obtained through dilated pupils. The

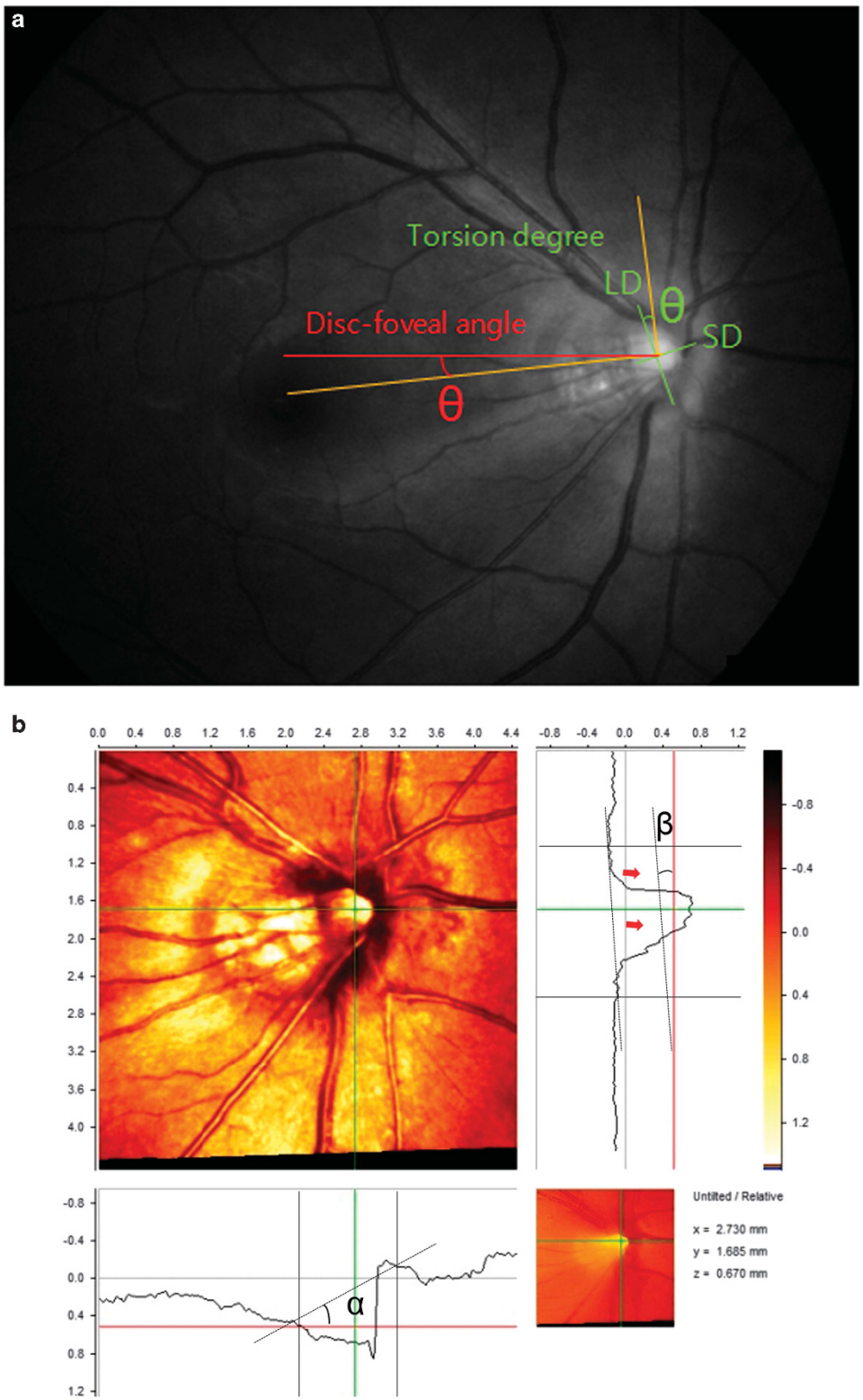

intrascan standard deviation was required to be $<30\,\mu$m. The extent of temporal and vertical tilt was measured from HRT printouts using the ImageJ software, as described previously.[19,23] Temporal disc tilt was defined as the tilt degree between a horizontal line and a line drawn manually to connect the two points where the height profile and disc margin met. Vertical disc tilt was defined as the angle between the vertical line and the line connecting the two points where the height profile and disc margin met. Positive horizontal and vertical disc tilt indicated the presence of temporal and inferior tilt, respectively.

OCT imaging of the lamina cribrosa

Horizontal and vertical cross-sectional B-scan images covering the optic disc, 30–34 μm apart, were obtained using the enhanced depth imaging (EDI) technique of the Spectralis OCT for LC analyses, described previously.[4,5,27] Images with a quality score higher than 15 were obtained ~65–70 sections per eye. The EDI OCT images were carefully reviewed for the presence of laminar holes or defects that violated the smooth curvilinear U- or W-shaped cross-sectional contour of the LC.[7,8,10,28,29] Experienced glaucoma specialists (HYS and YSH), blinded to the patients' clinical information and infrared optic disc photographs, performed this review.

Alteration of the LC was defined using the guidelines specified by Kiumehr *et al*[8] The LC alteration was considered to be present when focal LC defects, violating the curvilinear U- or W-shaped contour of the anterior LC surface, were observed. The diameter of the defects at their opening was required to be at least 100 μm in diameter and more than 30 μm in depth.[8] Additionally, to be considered as an LC alteration, the LC findings had to be present in two neighboring B-scans to avoid false positives.

The focal LC defects were classified by their location from the neural canal wall and the clock-hour location around the neural canal wall. The location of the focal LC defect was defined by Choi *et al*[11] A far-peripheral LC defect was defined as the defect being adjoined to the LC insertion, with the anterior LC visible on only the central side of the defect, and with the peripheral LC not visible due to masking by an overlying scleral rim (Figure 2—top). A mid-peripheral LC defect referred to a LC defect located within the center of the visible LC, with the LC visible on either side of the defect (Figure 2—middle). The clock-hour position of the LC defect was obtained from en face OCT images created by the built-in software of Spectralis (Figure 2—bottom). On the basis of the clock-hour sectors on the OCT, 12 30° clock-hour sectors were created. The locations of sectors were labeled 1 through 12, starting from the superonasal sector and running clockwise in the right eye and counterclockwise in the left eye. The LC defects located at the 6 and 7 clock-hour sectors, 11 and 12 clock-hour sectors, and 8–10 clock-hour sectors were defined as inferotemporal, superotemporal, and temporal LC defects, respectively. Focal LC defect overlying between two sectors was classified to the sector with the larger area of the focal LC defect located.

The depth of the anterior LC surface was determined by measuring the distance from Bruch's membrane opening plane to the level of the anterior LC surface. The line connecting the two termination points of Bruch's membrane edges was used as a reference plane for LC depth measurements at three points (from the vertical center of the reference line, and 100 μm temporally and nasally from the center of the reference line). The average of the three values was defined as the LC depth.

Classification of optic disc types

Two observers (HYP, CKP) classified the optic discs into four different groups according to the type of disc damage, using a modified process from previous research: notch, focal rim thinning, generalized rim thinning, and myopic optic disc.[30,31] Final decisions regarding disc damage type were based on the consensus of the two observers. A third glaucoma specialist (YSH) served as an adjudicator in cases of disagreement.

Figure 1 The posterior pole profiles and optic disc morphological features (disc tilt, disc torsion, disc-foveal angle, and tilt degree) were measured using disc and retinal nerve fiber layer photographs and Heidelberg Retina Tomograph (HRT) III images. (a) The disc tilt was determined using the disc ovality ratio. Disc ovality ratio was the ratio between the longest disc diameter (LD) and shortest disc diameter (SD) (green lines). Disc torsion refers to the deviation of the long disc (LD) axis from the vertical meridian (ie, the vertical line perpendicular to a reference line connecting the fovea and the disc center; yellow lines). The angle (green θ) between the vertical meridian and the long axis of the disc is the degree of torsion. The disc-foveal angle (red θ) is the angle between the optic disc and fovea as measured by the angle between the reference line (yellow line) and a horizontal line through the disc center (red line). (b) The degrees of temporal (α) and vertical (β) disc tilt were measured using HRT III. Temporal disc tilt (α) was defined as the tilt degree between a horizontal line (red line) and a line drawn manually to connect the two points where the height profile and disc margin met (black dotted line). Vertical disc tilt (β) was defined as the angle between the vertical line (red line) and the line connecting the two points where the height profile and disc margin met (black dotted line).

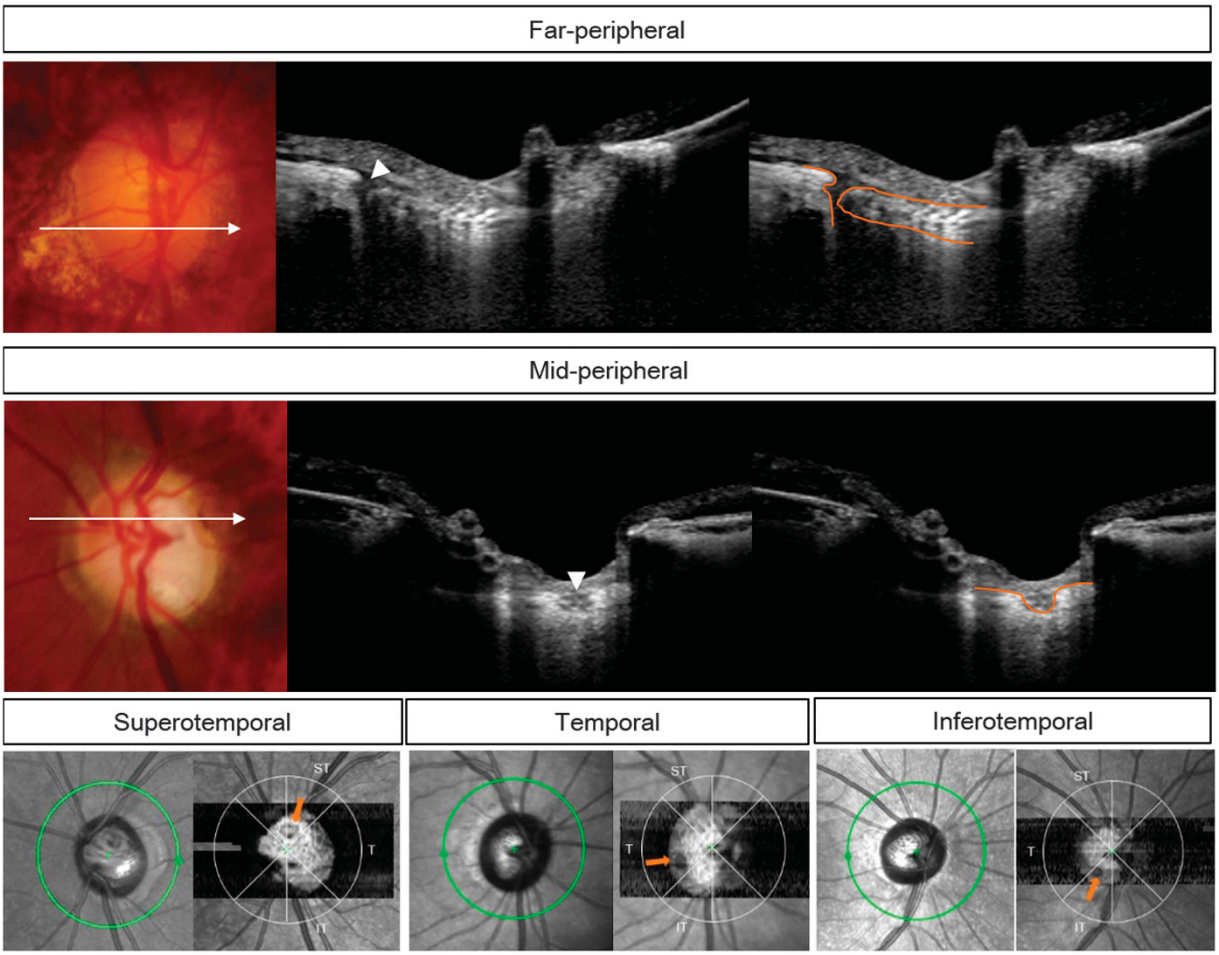

Figure 2 Classification of the alteration of lamina cribrosa (LC) from the B-scans of enhanced depth imaging of the optic disc and *en face* image. The white arrow shows the cross-sectional location of the B-scan, and the white arrowhead indicates the focal LC defect in each B-scan image. The orange line shows the anterior or posterior border of the LC. (top) The case shows far-peripheral LC defect, adjacent to the LC insertion. The LC is not visible peripheral to the defects. (bottom) The bottom case shows a mid-peripheral LC defect, havng visible LC on both side of the defect. The clock-hour position of the focal LC defect was obtained from *en face* images of the optical coherence tomography. On the basis the clock-hour sectors on the OCT, the focal LC defects located at the 6 and 7 clock-hour sectors, 11 and 12 clock-hour sectors, and 8–10 clock-hour sectors were defined as inferotemporal (IT), superotemporal (ST), and temporal (T) LC defects, respectively (orange arrow, indicating the focal LC defect).

Statistical analysis

Interobserver reproducibility of posterior profile parameter measurements was assessed by calculation of the intraclass correlation coefficients (ICCs). This was based on 30 randomly selected retinal photographs and HRT images. According to Fleiss,[32] ICC scores ≥ 0.75, between 0.40 and 0.75, and ≤ 0.4 are considered excellent, moderate, and poor, respectively. EDI OCT images of 30 randomly selected eyes were also evaluated to assess intraobserver and interobserver agreement on the presence of focal LC defects. Analysis was based on three independent series of re-evaluations. Kappa statistics of the presence of focal LC defects was used, and again scores ≥ 0.75, between 0.40 and 0.75, and ≤ 0.4 were considered to be excellent, moderate, and poor, respectively.[33]

Statistical analyses were performed using SPSS software (ver. 16.0; SPSS Inc., Chicago, IL, USA). Student's *t*-test and analysis of variance (ANOVA) with Scheffe's multiple comparison were used to compare data among the groups. The X^2-test or Fisher's exact test was used to analyze categorical variables. The level of statistical significance was set at $P<0.05$.

Results

A total of 184 eyes were enrolled from 184 open-angle glaucoma patients who met the inclusion and exclusion criteria. Out of these 184 eyes, 12 (6.5%) were excluded from further analysis, due to poor OCT scan images of the LC that did not offer information of the LC morphology

or poor visualization of the anterior LC < 70% of the horizontal scan length of the optic nerve head region due to prelaminar tissues or vessel shadows. The remaining 172 eyes were analyzed. Disc ovality ratio, torsion degree, PPA area, and tilt angle measurements, obtained from two observers, indicated moderate to excellent interobserver reproducibility. The interobserver mean ICC was 0.826 (0.711–0.864) for ovality ratio, 0.857 (0.738–0.879) for torsion degree, 0.844 (0.722–0.871) for PPA area, and 0.839 (0.719–0.869) for tilt angle. In addition, interobserver agreement in determining the presence or absence of a focal LC defect from OCT scanned images was excellent ($\kappa = 91.8$).

Out of the 172 eyes, 78 (45.3%) had far-peripheral LC defects, 28 (16.3%) had mid-peripheral LC defects, and the remaining 66 (38.4%) had no focal LC defects. Table 1 lists the clinical characteristics of each group. Eyes without focal LC defects had significantly higher untreated mean intraocular pressure (IOP), with the majority of them having a diagnosis of primary open-angle glaucoma (POAG; 90.7%), compared with eyes with focal LC defects ($P < 0.001$ and $P < 0.001$, respectively). Eyes with far-peripheral LC defects were from significantly younger patients (49.57 ± 13.41 years) with myopia (mean spherical equivalent, –4.01 ± 3.98 diopters; mean axial length, 25.34 ± 1.89 mm), compared with other groups ($P = 0.006$, $P = 0.005$, and $P < 0.001$, respectively).

Table 2 lists the characteristics of the anatomical characteristics of the optic disc. Eyes with far-peripheral LC defects frequently exhibited a myopic disc (73.1%),

Table 1 Demographic characteristics of open-angle glaucoma patients according to the findings of the lamina cribrosa detected by Spectralis optical coherence tomography using enhanced depth-imaging technique

	Eyes with far-peripheral LC defects (n = *78*)	*Eyes with mid-peripheral LC defects* (n = *28*)	*Eyes without focal LC defects* (n = *66*)	P-*value*[a]	P-*value*[b]
Age, years	49.57 ± 13.41	60.78 ± 9.38	54.39 ± 12.08	0.006[c]	0.012[c]
Gender, male:female	25:53	12:16	36:30	0.075[d]	0.107[d]
Central corneal thickness, μm	534.62 ± 31.70	538.50 ± 32.02	532.22 ± 30.78	0.822[c]	0.316[c]
Spherical equivalent, diopters	− 4.01 ± 3.98	− 1.47 ± 1.67	− 1.24 ± 2.61	0.005[c]	0.003[c]
Axial length, mm	25.34 ± 1.89	23.71 ± 0.96	24.03 ± 1.31	< 0.001[c]	0.012[c]
Untreated intraocular pressure, mmHg	16.62 ± 3.46	15.66 ± 2.64	25.45 ± 3.01	< 0.001[c]	< 0.001[c]
Average RNFL thickness, μm	78.19 ± 10.63	75.33 ± 11.14	75.21 ± 14.90	0.700[c]	0.830[c]
Mean deviation of VF, dB	− 6.64 ± 10.16	− 5.46 ± 4.11	− 5.38 ± 5.68	0.743[c]	0.897[c]
Diagnosis					
Normal-tension glaucoma, *n* (%)	42 (53.8%)	14 (50.0%)	6 (9.1%)	< 0.001[d]	0.826[d]
Primary open-angle glaucoma, *n* (%)	36 (46.2%)	14 (50.0%)	60 (90.9%)		

Abbreviations: LC, lamina cribrosa; RNFLD, retinal nerve fiber layer defect; VF, visual field. [a]Comparison between three groups. [b]Comparison between eyes with far-peripheral and mid-peripheral LC defects. [c]One-way ANOVA with multiple comparison. [d]X^2-test.

Table 2 Characteristics of the posterior pole profiles including the optic disc morphology according to the findings of the lamina cribrosa detected by Spectralis optical coherence tomography using enhanced depth imaging technique

	Eyes with far-peripheral LC defects (n = *78*)	*Eyes with mid-peripheral LC defects* (n = *28*)	*Eyes without focal LC defects* (n = *66*)	P-*value*[a]	P-*value*[b]
Characteristics of the optic disc					
Morphological features					
Notch or focal rim thinning	16 (20.5%)	14 (50.0%)	16 (24.2%)	< 0.001[d]	< 0.001[d]
Generalized rim thinning	5 (6.4%)	10 (35.7%)	40 (60.6%)		
Myopic	57 (73.1%)	4 (14.3%)	10 (15.2%)		
Disc tilt, *n* (%)	24 (30.8%)	4 (14.3%)	4 (6.1%)	0.009[d]	0.133[d]
Ovality ratio	1.33 ± 0.19	1.14 ± 0.10	0.12 ± 0.10	< 0.001[c]	0.041[c]
Disc torsion, *n* (%)	29 (37.2%)	12 (42.9%)	12 (18.2%)	0.116[d]	0.654[d]
Torsion degree, degree	5.02 ± 24.26	-6.51 ± 19.22	-1.69 ± 18.17	0.082[c]	0.452[c]
Peripapillary atrophy area, pixel area	10321.4 ± 10664.5	7853.4 ± 16168.4	5284.7 ± 5919.5	0.067[c]	0.718[c]
Disc-foveal angle, degree	8.34 ± 3.31	12.15 ± 4.02	8.43 ± 3.03	0.001[c]	0.001[c]
Characteristics of the LC alterations					
Location of LC defects, clock-hour	8.61 ± 1.20	8.14 ± 1.46			0.195[c]
LC depth, μm	422.89 ± 115.22	426.00 ± 76.58	498.24 ± 127.10	0.028[c]	0.996[c]

Abbreviation: LC, lamina cribrosa. [a]Comparison between three groups. [b]Comparison between eyes with far-peripheral and mid-peripheral LC defects. [c]One-way ANOVA with multiple comparison. [d]X^2-test.

with predominant disc tilt (30.8%) and a higher ovality ratio (1.33 ± 0.19), compared with the other groups. The optic disc of eyes with mid-peripheral LC defects had frequent focal changes, such as notch or focal rim thinning (50.0%). In eyes with mid-peripheral LC defects, the disc-foveal angle (12.15 ± 4.02°) was significantly greater than in other groups ($P = 0.001$). Eyes without focal LC defects had generalized rim thinning as the most frequent optic disc morphology (60.6%); in this case, the LC depth (498.24 ± 127.10 μm) was significantly greater than in eyes with LC defects ($P = 0.028$). The clock-hour location of LC defects did not differ significantly between eyes with far-peripheral and mid-peripheral LC defects ($P = 0.195$).

Out of the 106 eyes with a focal LC defect, 26 (24.6%) were located in the superotemporal region, 31 (29.2%) in the temporal region, and 49 (46.2%) in the inferotemporal region. Eyes with superotemporal and temporal LC defects had significantly more frequent disc tilt, compared with eyes with inferotemporal LC defects ($P = 0.018$; Table 3). Disc tilt degree by HRT revealed significant temporal disc tilt in eyes with temporal LC defects, compared with the other groups ($P < 0.001$). No significant differences were observed in the vertical disc tilt degree between groups. Eyes with inferotemporal LC defects had a significantly larger disc-foveal angle compared with the other groups ($P = 0.027$).

Discussion

The results of the present study can be summarized as follows. (1) Eyes without a focal LC defect had higher baseline untreated IOP, with mainly POAG as the diagnosis. The LC findings in this group were characterized by a deep LC depth. (2) Eyes with a focal LC defect located at the far-peripheral region of the disc were myopic. (3) Eyes with focal LC defects located at the temporal region of the disc had a greater temporal disc tilt degree, compared with eyes with LC defects at other clock-hour locations and were myopic eyes. (4) Focal LC defects located at the mid-peripheral region or at an inferotemporal position had a significantly larger disc-foveal angle.

The finding that eyes without a focal LC defect had a high IOP with deep location of the anterior LC surface is consistent with previous findings that the posterior location of the anterior LC surface is related to high IOP.[34–36] We also found that LC depth was correlated with initially untreated IOP in our previous study.[37] IOP reduction reverses the posterior displacement of the LC.[4,38,39] Optic disc morphological characteristics of the eyes without a focal LC defect included generalized rim enlargement, which may also be related to the deep LC depth from a high IOP. POAG is reported to exhibit diffuse damage in the RNFL and VF, compared with NTG.[40–46] These findings suggest that the backward bowing and posterior location of the LC by high IOP may be related to the pathogenic mechanism of glaucomatous damage in POAG. In contrast, focal LC defects are localized changes of the LC. Focal laminar defects are associated with localized RNFL defects, disc hemorrhages, NTG diagnosis, myopia, and paracentral scotomas.[7–12] NTG displays more localized, deep damage, which is closer to the macula, compared with POAG.[40–46] Research has shown that these characteristics of NTG could be related to focal LC defects in some eyes.

Table 3 Characteristics of the optic disc morphology and the characteristics of the lamina cribrosa defects by the clock-hour location of the lamina cribrosa defect

	LC defect at superotemporal region (n = *26*)	*LC defect at temporal region* (n = *31*)	*LC defect at inferotemporal region* (n = *49*)	P-*value*	*Multiple comparison*
Characteristics of the LC alterations					
Far-peripheral LC defects, *n* (%)	20 (76.9%)	29 (93.5%)	36 (73.5%)	0.241[a]	T > S = I
Mid-peripheral LC defects, *n* (%)	6 (23.1%)	2 (6.5%)	13 (26.5%)		
Location of LC defects					
Clock hour position	11.18 ± 0.39	9.00 ± 0.26	7.25 ± 0.49	< 0.001[b]	S > T > I
Characteristics of the optic disc					
Disc tilt, *n* (%)	11 (42.3%)	12 (38.7%)	7 (14.2%)	0.018[a]	S = T > I
Ovality ratio	1.32 ± 0.22	1.28 ± 0.13	1.18 ± 0.17	0.050[b]	S = T > I
Temporal disc tilt, degree	7.23 ± 6.16	13.23 ± 5.84	7.12 ± 6.08	< 0.001[b]	T > S = I
Inferior disc tilt, degree	3.26 ± 3.86	3.54 ± 3.41	1.26 ± 2.56	0.380[b]	
Disc torsion, *n* (%)	11 (42.3%)	15 (48.4%)	13 (26.5%)	0.214[a]	S = T > I
Torsion degree, degree	6.99 ± 28.63	8.54 ± 24.45	-3.02 ± 19.08	0.091[b]	S = T > I
Peripapillary atrophy area, pixel area	12177.5 ± 12937.25	12343.5 ± 15332.07	6781.0 ± 5085.6	0.079[b]	S = T > I
Disc-foveal angle, degree	7.59 ± 3.32	8.45 ± 3.63	10.05 ± 3.62	0.027[b]	S < T < I

Abbreviation: LC, lamina cribrosa. [a]X^2-test. [b]One-way ANOVA with multiple comparison.

Park proposed that structural changes in the LC in glaucoma patients could occur in both a generalized and localized fashion.[6] Our findings suggest that generalized change (eg, a deep LC depth without focal LC defects) could be a response to high IOP. Localized LC changes could occur in both POAG and NTG. However, unlike generalized posterior displacement or deepening of the LC depth, focal LC defects may represent regional susceptibility and regional deformation of the LC.

The focal LC defects were located at the far-peripheral or mid-peripheral LC depending on their location with respect to the neural canal wall. We found that far-peripheral LC defects were more frequent than mid-peripheral LC defects, which is consistent with previous findings.[7,8,11] Choi *et al* suggested that far-peripheral LC defects may represent tissue discontinuity between the LC and the sclera or posterior migration of the LC.[11] Kiumehr *et al* suggested a disruption of the laminar insertion site, due to the relatively large mechanical strain in the peripheral LC.[8] Recent investigations have found that temporal disc tilt is related to the presence of LC defects in myopic eyes.[12,47] Our study adds the important findings that focal LC defects in myopic eyes are located in the far-peripheral region and at the temporal clock-hour position. Focal LC defects located in the temporal region were correlated with the temporal disc tilt degree, suggesting that the formation of focal LC defects in the temporal region of myopic eyes may be associated with temporal stretching of the optic disc by axial elongation of the eyeball. In this case, localized LC changes may be the result of a myopic change in the posterior segment of the eye and around the optic disc. This site could serve as a weak point for glaucomatous changes in patients with myopic glaucoma. The focal LC defects found in locations other than the inferotemporal region could be related to changes in the ocular posterior segment and related optic disc morphological changes (temporal optic disc tilt in our study), which may contribute as a region that is susceptible to glaucomatous changes.

Knowing the ocular characteristics related to the location of focal LC defects may be important clinically, since eyes with LC defects tended to progress faster than eyes without LC defects.[48] Eyes with focal LC defects in the superotemporal or temporal regions were myopic eyes with significant disc tilt and torsion compared with eyes with focal LC defects in the inferotemporal regions. In contrast, eyes with focal inferotemporal LC defects, the disc-foveal angle was significantly larger. Eyes with a larger disc-foveal angle are reported to have frequent superior central VF defects.[17] The inferior foveal location relative to the optic disc results in a distinct asymmetric distribution of the RNFL between the superior and inferior retina, particularly in papillomacular bundle fibers originating from the central retina. As Hood explained, this causes crowding of the papillomacular bundles at the inferotemporal disc at the level of the LC and this may contribute to the regional susceptibility of the inferotemporal LC.[49] For eyes with focal LC defects in the inferotemporal region, the LC defect may serve as a site of progression and have more important clinical importance than LC defects in other locations.

Our study had several limitations that must be acknowledged. One limitation is the poor visualization of the LC under the optic disc rim and vessels. It is possible that some LC alterations in area with poor OCT penetration may have been missed. The classification of far-peripheral and mid-peripheral LC defects was based on the visible portions of the LC. Some far-peripheral LC defects could have been considered as mid-peripheral LC defects, but the peripheral portion of the LC was not captured. To reduce false-positive detection of focal LC defects, we defined a LC defect as having a diameter at least 100 μm and a depth of more than 30 μm. The LC defect also had to be present in two neighboring B-scans both in the horizontal and vertical scans. The definition of LC defects were based on previous studies; however, there could be controversies in the definition. Myopic eyes and glaucomatous eyes tend to have thinner LC and the visibility of the LC could be enhanced in these eyes resulting potential bias to the study.

In conclusion, our results indicate that the location of the focal LC defect may have different clinical significance. Far-peripheral LC defects located in the temporal region of the optic disc were frequently found in myopic glaucomatous eyes. Eyes with focal LC defects located at the mid-peripheral and inferotemporal locations had a larger disc-foveal angle, suggesting contribution of the LC to the pathogenesis of glaucoma.

Summary

What was known before

- Structural alterations at the level of the lamina cribrosa (LC) are important in the pathogenesis of glaucoma. LC findings including LC thinning, posterior displacement, and changes like focal hole, focal defect, and disinsertion. The clinical relevance of the presence of LC findings and the location of these LC findings has yet to be determined.

What this study adds

- Eyes with far-peripheral LC defects in the temporal region were significantly myopic and had a higher disc ovality ratio. Eyes with inferotemporal LC defects had a significantly larger disc-foveal angle. The location of the LC defects are related to several clinical characteristics.

Conflict of interest

The authors declare no conflict of interest.

Acknowledgements

This research was supported by Basic Science Research Program through the National Research Foundation of Korea (NRF) funded by the Ministry of Education (2016R1A6A1A03010528).

References

1 Morrison JC, Jerdan JA, Dorman ME, Quigley HA. Structural proteins of the neonatal and adult lamina cribrosa. *Arch Ophthalmol* 1989; **107**(8): 1220–1224.
2 Morrison JC, L'Hernault NL, Jerdan JA, Quigley HA. Ultrastructural location of extracellular matrix components in the optic nerve head. *Arch Ophthalmol* 1989; **107**(1): 123–129.
3 Burgoyne CF. A biomechanical paradigm for axonal insult within the optic nerve head in aging and glaucoma. *Exp Eye Res* 2011; **93**: 120–132.
4 Park HY, Shin HY, Jung KI, Park CK. Changes in the lamina and prelamina after intraocular pressure reduction in patients with primary open-angle glaucoma and acute primary angle-closure. *Invest Ophthalmol Vis Sci* 2014; **55**(1): 233–239.
5 Park HY, Jeon SH, Park CK. Enhanced depth imaging detects lamina cribrosa thickness differences in normal tension glaucoma and primary open-angle glaucoma. *Ophthalmology* 2012; **119**(1): 10–20.
6 Park SC. In vivo evaluation of lamina cribrosa deformation in glaucoma. *J Glaucoma* 2013; **22**(Suppl 5): S29–S31.
7 Park SC, Hsu AT, Su D, Simonson JL, Al-Jumayli M, Liu Y *et al.* Factors associated with focal lamina cribrosa defects in glaucoma. *Invest Ophthalmol Vis Sci* 2013; **54**(13): 8401–8407.
8 Kiumehr S, Park SC, Syril D, Teng CC, Tello C, Liebmann JM *et al. In vivo* evaluation of focal lamina cribrosa defects in glaucoma. *Arch Ophthalmol* 2012; **1305**: 552–559.
9 You JY, Park SC, Su D, Teng CC, Liebmann JM, Ritch R. Focal lamina cribrosa defects associated with glaucomatous rim thinning and acquired pits. *JAMA Ophthalmol* 2013; **131**(3): 314–320.
10 Tatham AJ, Miki A, Weinreb RN, Zangwill LM, Medeiros FA. Defects of the lamina cribrosa in eyes with localized retinal nerve fiber layer loss. *Ophthalmology* 2014; **121**(1): 110–118.
11 Choi YJ, Lee EJ, Kim BH, Kim TW. Microstructure of the optic disc pit in open-angle glaucoma. *Ophthalmology* 2014; **121**(11): 2098–2106.e2092.
12 Kimura Y, Akagi T, Hangai M, Takayama K, Hasegawa T, Suda K *et al.* Lamina cribrosa defects and optic disc morphology in primary open angle glaucoma with high myopia. *PloS One* 2014; **9**(12): e115313.
13 Qayum S, Sullivan T, Park SC, Merchant K, Banik R, Liebmann JM *et al.* Structure and clinical significance of central optic disc pits. *Ophthalmology* 2013; **120**(7): 1415–1422.
14 Takayama K, Hangai M, Kimura Y, Morooka S, Nukada M, Akagi T *et al.* Three-dimensional imaging of lamina cribrosa defects in glaucoma using swept-source optical coherence tomography. *Invest Ophthal Vis Sci* 2013; **54**(7): 4798–4807.
15 Shin HY, Park HY, Park CK. The effect of myopic optic disc tilt on measurement of spectral-domain optical coherence tomography parameters. *Br J Ophthalmol* 2015; **99**(1): 69–74.
16 Choi JA, Park HY, Shin HY, Park CK. Optic disc tilt direction determines the location of initial glaucomatous damage. *Invest Ophthalmol Vis Sci* 2014; **55**(8): 4991–4998.
17 Choi JA, Park HY, Park CK. Difference in the posterior pole profiles associated with the initial location of visual field defect in early-stage normal tension glaucoma. *Acta Ophthalmol* 2014; **93**: 598–625.
18 Choi JA, Park HY, Shin HY, Park CK. Optic disc characteristics in patients with glaucoma and combined superior and inferior retinal nerve fiber layer defects. *JAMA Ophthalmol* 2014; **132**(9): 1068–1075.
19 Choi JA, Kim JS, Park HY, Park H, Park CK. The foveal position relative to the optic disc and the retinal nerve fiber layer thickness profile in myopia. *Invest Ophthalmol Vis Sci* 2014; **55**(3): 1419–1426.
20 Park HY, Lee K, Park CK. Optic disc torsion direction predicts the location of glaucomatous damage in normal-tension glaucoma patients with myopia. *Ophthalmology* 2012; **119**(9): 1844–1851.
21 Giuffre G. Chorioretinal degenerative changes in the tilted disc syndrome. *Int Ophthalmol* 1991; **15**(1): 1–7.
22 Vongphanit J, Mitchell P, Wang JJ. Population prevalence of tilted optic disks and the relationship of this sign to refractive error. *Am J Ophthalmol* 2002; **133**(5): 679–685.
23 Tay E, Seah SK, Chan SP, Lim AT, Chew SJ, Foster PJ *et al.* Optic disk ovality as an index of tilt and its relationship to myopia and perimetry. *Am J Ophthalmol* 2005; **139**(2): 247–252.
24 Samarawickrama C, Mitchell P, Tong L, Gazzard G, Lim L, Wong TY *et al.* Myopia-related optic disc and retinal changes in adolescent children from singapore. *Ophthalmology* 2011; **118**(10): 2050–2057.
25 How AC, Tan GS, Chan YH, Wong TT, Seah SK, Foster PJ *et al.* Population prevalence of tilted and torted optic discs among an adult Chinese population in Singapore: the Tanjong Pagar Study. *Arch Ophthalmol* 2009; **127**(7): 894–899.
26 Takasaki H, Higashide T, Takeda H, Ohkubo S, Sugiyama K. Relationship between optic disc ovality and horizontal disc tilt in normal young subjects. *Jpn J Ophthalmol* 2013; **57**(1): 34–40.
27 Park HY, Park CK. Diagnostic capability of lamina cribrosa thickness by enhanced depth imaging and factors affecting thickness in patients with glaucoma. *Ophthalmology* 2013; **120**(4): 745–752.
28 Choi YJ, Lee EJ, Kim BH, Kim TW. Microstructure of the optic disc pit in open-angle glaucoma. *Ophthalmology* 2014; **121**(11): 2098–2106.e3.
29 Lee EJ, Kim TW, Kim M, Girard MJ, Mari JM, Weinreb RN. Recent structural alteration of the peripheral lamina cribrosa near the location of disc hemorrhage in glaucoma. *Invest Ophthalmol Vis Sci* 2014; **55**(4): 2805–2815.
30 Nicolela MT, Drance SM. Various glaucomatous optic nerve appearances: clinical correlations. *Ophthalmology* 1996; **103**(4): 640–649.
31 Shin HY, Park HY, Jung Y, Choi JA, Park CK. Glaucoma diagnostic accuracy of optical coherence tomography parameters in early glaucoma with different types of optic disc damage. *Ophthalmology* 2014; **121**(10): 1990–1997.
32 Fleiss JL. *The Design and Analysis of Clinical Experiments*. Wiley: New York, 1986.
33 Fleiss J, Levin B, Paik M. The measurement of interrate agreement. In: Shewart WA, Wilks SS (eds). *Statistical*

Methods for Rates and Proportions. Wiley-Intersicence. Wiley: New Jersey, USA, 2003, pp 598-625.

34 Lee KM, Kim TW, Weinreb RN, Lee EJ, Girard MJ, Mari JM. Anterior lamina cribrosa insertion in primary open-angle glaucoma patients and healthy subjects. *PloS One* 2014; **9**(12): e114935.

35 Furlanetto RL, Park SC, Damle UJ, Sieminski SF, Kung Y, Siegal N *et al.* Posterior displacement of the lamina cribrosa in glaucoma: *in vivo* interindividual and intereye comparisons. *Invest Ophthalmol Vis Sci* 2013; **54**(7): 4836–4842.

36 Yan DB, Coloma FM, Metheetrairut A, Trope GE, Heathcote JG, Ethier CR. Deformation of the lamina cribrosa by elevated intraocular pressure. *Br J Ophthalmol* 1994; **78**(8): 643–648.

37 Jung KI, Jung Y, Park KT, Park CK. Factors affecting plastic lamina cribrosa displacement in glaucoma patients. *Invest Ophthalmol Vis Sci* 2014; **55**(12): 7709–7715.

38 Yoshikawa M, Akagi T, Hangai M, Ohashi-Ikeda H, Takayama K, Morooka S *et al.* Alterations in the neural and connective tissue components of glaucomatous cupping after glaucoma surgery using swept-source optical coherence tomography. *Invest Ophthalmol Vis Sci* 2014; **55**(1): 477–484.

39 Lee EJ, Kim TW, Weinreb RN. Reversal of lamina cribrosa displacement and thickness after trabeculectomy in glaucoma. *Ophthalmology* 2012; **119**(7): 1359–1366.

40 Kim DM, Seo JH, Kim SH, Hwang SS. Comparison of localized retinal nerve fiber layer defects between a low-teen intraocular pressure group and a high-teen intraocular pressure group in normal-tension glaucoma patients. *J Glaucoma* 2007; **16**(3): 293–296.

41 Yamazaki Y, Koide C, Miyazawa T, Kuwagaki N, Yamada H. Comparison of retinal nerve-fiber layer in high- and normal-tension glaucoma. *Graefes Arch Clin Exp Ophthalmol* 1991; **229**(6): 517–520.

42 Kubota T, Khalil AK, Honda M, Ito S, Nishioka Y, Inomata H. Comparative study of retinal nerve fiber layer damage in Japanese patients with normal- and high-tension glaucoma. *J Glaucoma* 1999; **8**(6): 363–366.

43 Gramer E, Althaus G, Leydhecker W. Site and depth of glaucomatous visual field defects in relation to the size of the neuroretinal edge zone of the optic disk in glaucoma without hypertension, simple glaucoma, pigmentary glaucoma. A clinical study with the Octopus perimeter 201 and the optic nerve head analyzer. *Klin Monatsbl Augenheilkd* 1986; **189**(3): 190–198.

44 Caprioli J, Spaeth GL. Comparison of visual field defects in the low-tension glaucomas with those in the high-tension glaucomas. *Am J Ophthalmol* 1984; **97**(6): 730–737.

45 Caprioli J, Spaeth GL. Comparison of the optic nerve head in high- and low-tension glaucoma. *Arch Ophthalmol* 1985; **103**(8): 1145–1149.

46 Hitchings RA, Anderton SA. A comparative study of visual field defects seen in patients with low-tension glaucoma and chronic simple glaucoma. *Br J Ophthalmol* 1983; **67**(12): 818–821.

47 Shoji T, Kuroda H, Suzuki M, Baba M, Hangai M, Araie M *et al*. Correlation between lamina cribrosa tilt angles, myopia and glaucoma using OCT with a wide bandwidth femtosecond mode-locked laser. *PloS One* 2014; **9**(12): e116305.

48 Faridi OS, Park SC, Kabadi R, Su D, De Moraes CG, Liebmann JM *et al.* Effect of focal lamina cribrosa defect on glaucomatous visual field progression. *Ophthalmology* 2014; **121**(8): 1524–1530.

49 Hood DC, Raza AS, de Moraes CG, Liebmann JM, Ritch R. Glaucomatous damage of the macula. *Prog Retin Eye Res* 2013; **32**: 1–21.